Received: 24 October 2022 | Revised: 10 January 2023 | Accepted: 11 January 2023

DOI: 10.1002/app.53672

RESEARCH ARTICLE

Applied Polymer SCIENCE WILEY

Novel poly(ester amide) derived from tyrosine amino acid for targeted pulmonary drug delivery of fluticasone propionate

Hussien AbdulKarim[1] | **Dalia K. Ali**[2] | **Esra' Taybeh**[1] | **Hamad S. Alyami**[3] | **Shereen M. Assaf**[4] | **Eman Zmaily Dahmash**[5]

[1]Department of Applied Pharmaceutical Sciences and Clinical Pharmacy, Faculty of Pharmacy, Isra University, Amman, Jordan

[2]Department of Physiotherapy, Faculty of Allied Medical Sciences, Isra University, Amman, Jordan

[3]Department of Pharmaceutics, College of Pharmacy, Najran University, Najran, Saudi Arabia

[4]Department of Pharmaceutical Technology, Faculty of Pharmacy, Jordan University of Science and Technology, Irbid, Jordan

[5]Department of Chemistry and Pharmaceutical Sciences, School of Life Sciences, Pharmacy and Chemistry, Kingston University, London, UK

Correspondence
Eman Zmaily Dahmash, Kingston University, London KT1 2EE, UK.
Email: e.dahmash@kingston.ac.uk

Abstract

Nanoaggregates made from amino acid-based polymers have been an important platform for targeted drug delivery systems such as the lungs. Therefore, the aim of the present study is to develop tyrosine-based poly(ester amide)s (Tyr-PEA) for dry powder inhaler (DPI) of a potent drug (fluticasone propionate [FP]) using interfacial polymerization. The molecular and surface profiling characteristics were evaluated using Fourier-transformed infrared spectroscopy, X-ray diffraction, transmission electron microscopy, particle size analysis, nuclear magnetic resonance, differential scanning calorimetry, and scanning electron micrographs. The aerodynamic performance was evaluated using the NGI. The results confirmed the formation of the PEA and FP-loaded Tyr-PEA with an average particle size of, 45.39 ± 6.32 nm. The produced FP/Tyr-PEA showed entrapment efficiency and encapsulation capacity of FP of 92.32% and 0.526% respectively, which enabled the delivery of this potent drug in a reasonable dose. The in-vitro performance of the FP-loaded PEA was compared to a marketed product and results revealed a significant enhancement of the emitted dose (87.29% vs. 59% respectively [t-test, $p < 0.05$]). FP-loaded Tyr-PEA produced a higher respirable dose when compared to the marketed FP DPI (48.63 μg vs. 34.15 μg). Overall, FP-loaded Tyr-PEA was successfully prepared with optimal performance. Tyr-PEA-based nanoparticles provide a potential platform for targeted drug delivery, particularly potent actives.

KEYWORDS

dry powder inhaler, fluticasone propionate, interfacial polymerization, nanoparticles, poly (ester amide), respiratory drug delivery, tyrosine

1 | INTRODUCTION

Biodegradable and biocompatible polymeric materials are continually increasing and evolving for biomedical applications owing to their optimized properties and their biocompatible degradation products that are nontoxic or are eliminated from the body through natural metabolic pathways.[1,2]

Polymers used in biomedicine are derived from natural origin such as carrageenan, chitosan, gelatin, and hyaluronic acid.[3] They can also be manufactured from biocompatible compounds such as poly(lactic-co-glycolic acid) (PLGA), poly(glycolic acid) (PGA) and poly(lactic acid) (PLA). Although natural polymers are abundant in nature and biocompatible, synthetic polymers show great synthesizing flexibility and reproducibility which are often required in commercial applications.[4]

Poly (ester amide)s (PEAs) are a family of synthetic polymers whose structure includes both ester and amide linkages. The PEAs properties lie between polyesters and polyamides. Intra- and intermolecular hydrogen bonding is promoted by amide linkage, which provides good mechanical and thermal properties of the PEAs, while ester linkage enhances the biodegradability of the PEAs. Recently, α-amino acid-based PEAs have been investigated as a potential group of biodegradable polymers due to good processing properties, and susceptibility to both hydrolytic and enzymatic degradation.[5] Upon degradation, α-amino acid-based PEAs due to their natural origin release metabolites in the human body (α-amino acids), which are nontoxic. They also, protect cells from potential reduction in local pH which often happens due to polyester degradation; the degradation products of PEAs have both acid and essential natures, and thus a neutralization effect occurs. Another advantage of PEAs derived from α-amino acids is that it can be targeted for cleavage by proteolytic enzymes.[6]

Earliest attempts to synthesize and characterize PEAs were based on α-amino acids glycine, L- and L,D-alanine, L-phenylalanine and L-methionine.[7] In this study, we report the synthesis of PEAs derived from L-tyrosine. L-tyrosine is a naturally occurring amino acid that contains a phenolic hydroxyl group. Because of this feature, tyrosine can react as monomer; a building block in biodegradable polymers such as Tyrosine-based poly(amino acids), tyrosine-based polycarbonates, polyacrylates, and polyesters. The polymerization of a monomer is fast, easily scalable, and an efficient entrapment method of drug encapsulation using biodegradable polymers.[8] For instance, interfacial polymerization has advantages of having high-efficiency drug encapsulation and spontaneous polymer-nanoparticle formation.[9]

Nanoparticles made with biodegradable polymers have been an important platform on which therapeutic molecules are coupled, functionalized, coated, or entrapped in different devices aimed to control the drug release into specific sites in the body.[10,11] Currently, biodegradable polymeric nanoparticles serve as delivery systems for drugs used in the treatment of different illnesses such as respiratory diseases.[12]

In respiratory diseases, the main medication group that is used in controlling persistent asthma and reducing airway inflammation and bronchial hyper responsiveness is corticosteroids (CS)s. The effect of CSs for the

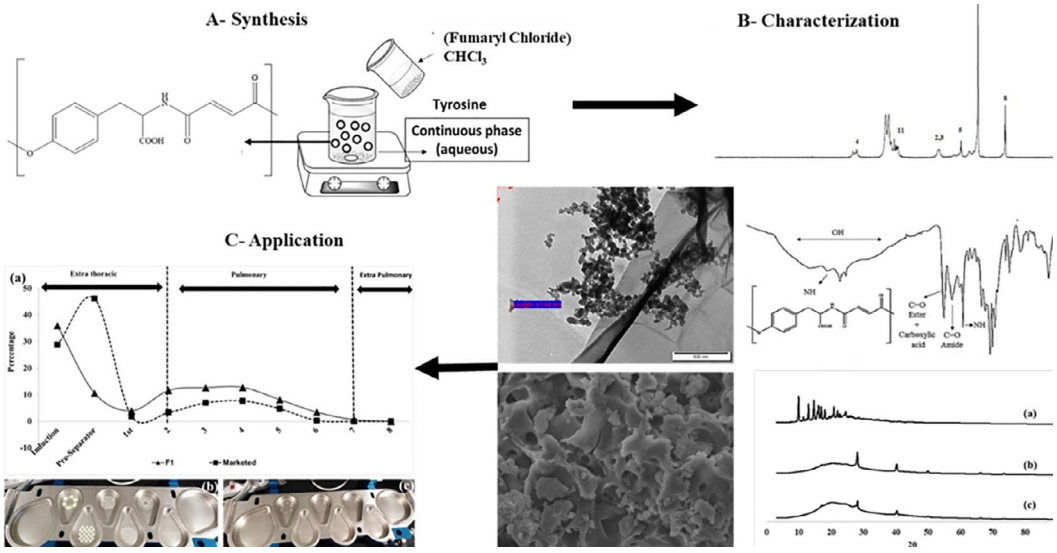

SCHEME 1 Schematic diagram for the synthesis and characterization of FP loaded Tyr-PEAs using interfacial polymerization techniques to target pulmonary drug delivery of FP [Color figure can be viewed at wileyonlinelibrary.com]

treatment of asthma in children was clearly explored throughout the literature and they are classified as the first line treatment of persistent asthma in children.[13] However, inhaled corticosteroid (ICS) rather than systemic CS use in asthma treatment is the ideal route of drug administration for children since local delivery of drug through inhalation has several advantages of providing a rapid onset of action, higher bioavailability, with lower needed doses and less side-effects than other routes.[14] Fluticasone propionate (FP), a synthetic ICS, with either low (50–100 mcg), medium (100–200 mcg) or high dose (>200 mcg), is one of the most widely used medications for the treatment of persistent asthma in children.[15] The high efficacy of FP is related to its effect on down regulation of pro-inflammatory proteins and on reversing of the asthma-induced airway remodeling.[16]

Dry powder inhaler (DPI) is a good option for FP delivery in children with asthma since it may help to overcome several limitations that are associated with other types of inhalation delivery systems (e.g., accuracy and reproducibility of the dose delivered, compliance and adherence issues, and environmental aspects).[17] However, a novel targeting agent is required to provide adequate drug concentrations and retain drugs within the lung, sustained effects, with minimal systemic absorption and undesired side effects.[18] Therefore, biodegradable polymeric nanoparticles have been used in the formulation of DPIs. To enable better delivery DPIs are usually formulated with a large nonrespirable carrier which magnifies the powder and helps in efficient dose metering. On actuation, therapeutic molecules along with the carrier gets dispersed into the patient mouth but only the respirable therapeutic molecules will reach the respiratory tract. The large nonrespirable carrier particles separate and deposit on the oropharynx and is swallowed in to the gastrointestinal tract. The choice of nonrespirable carrier for DPI formulation is critical. Lactose carrier, for example, has historical precedence and has an FDA approval for DPI use but its usage is limited due to patient lactose intolerance and allergies.[17] Therefore, other nonrespirable carriers such as biodegradable polymers can be proposed as potential carriers that can be used for DPI. The present work focused on preparing of a new formula containing PEAs based on tyrosine amino acid carrier of FP (Scheme 1). Due to the importance of this class of polymer in biomedical applications, it was worthwhile to investigate the use of this biodegradable polymer synthesized by interfacial polymerization with controlled surface functionality as a carrier in DPI for the pulmonary delivery of FP for the treatment of asthma in children.

2 | MATERIALS AND METHODS

2.1 | Materials

FP ($C_{25}H_{31}F_3O_5C$) was supplied by Discovery Fine Chemicals (Windborne, United Kingdom), possessing a molecular weight (MW) of 500.57 g/mol. Fumaryl chloride was purchased from Fisher Scientific (Waltham, MA, USA). Methyl alcohol was supplied from Tedia high purity solvent (Fairfield, Ohio, USA). Chloroform ($CHCl_3$), Acetonitrile HPLC grade (CH_3CN) MW (41.05 g/mol), Trifluoroacetic Acid (TFA) ($C_2HF_3O_2$) MW 114.02 g/mol, and HPLC grade water (H_2O) MW (18.02 g/mol), and diethyl ether were purchased from alpha Chemika (India). Tyrosine was purchased from Sigma (Pool, UK).

2.2 | Synthesis of poly(ester amide) based on tyrosine

A mixture of the amino acid tyrosine (1.82 g, 10 mmol) and KOH (1.12 g, 20 mmol) was dissolved in distilled water (30 ml). A fumaryl chloride solution (1.52 g, 10 mmol) dissolved in $CHCl_3$ (10 ml) was added dropwise to the aqueous solution under vigorous stirring. The reaction was allowed to proceed under vigorous stirring for 15 min. The formed polymer was filtered off and washed several times with distilled water and diethyl ether. The last traces of solvent were removed by keeping the polymer in a freeze dryer for 6 h. The produced powder was sieved using a 32 μm sieve. After that, the formula was collected and stored at room temperature.

2.3 | Synthesis of FP loaded poly(ester amide)s based on tyrosine

A mixture of the amino acid tyrosine (1.82 g, 10 mmol) and KOH (1.12 g, 20 mmol) was dissolved in distilled water (30 ml). A fumaryl chloride solution (1.52 g, 10 mmol) and 10 mg of FP dissolved in $CHCl_3$ (10 ml) were added dropwise to the aqueous solution under vigorous stirring. The reaction was allowed to proceed under vigorous stirring for 15 min (see Figure 1). The polymer formed was filtered off and washed several times with distilled water and diethyl ether. The last traces of solvent were removed by keeping the polymer in a freeze dryer for 6 h. The produced powder was sieved using a 32 μm sieve. After that, the formula was collected and stored at room temperature.

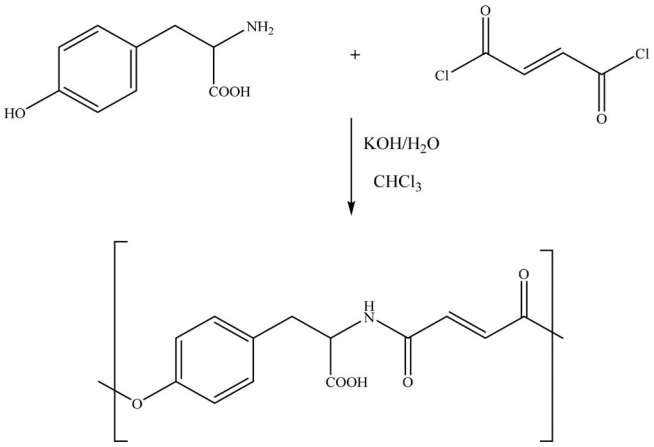

FIGURE 1 Synthesis of new PEAs based on tyrosine

2.4 | FP quantification and validation using HPLC analytical method

FP is classified as a second-generation trifluorinated glucocorticosteroid based on the androstane nucleus. Although FP is a water insoluble compound, the solubility of FP in water is around 0.39% may affect its absorption and effectiveness. Therefore, a previously reported simple method for the analysis of FP using HPLC with a UV detector has been employed with modification in the present study.[19]

HPLC analysis was performed using DionexUltiMate® 3000 from Thermo Fisher Scientific™ (USA). The chromatographic separation was achieved using a 5 μm C18 (250*4.6 mm) column from Fortis Technologies Ltd, UK. The mobile phase was made of acetonitrile: 0.125% TFA in water with a ratio of 85:15. The run time was 8 min. The column temperature was set as 20°C, the sample temperature was off, and the UV detection wavelength was set at 239 nm. The sample volume was 20 μl for each sample, and the flow rate was 1 ml/min. The method was validated according to the International Council for Harmonization (ICH) guidelines (Q2 [R1] [2005] Validation of analytical procedures: Text and methodology Q2[R1]).[20] A stock solution of FP was prepared by dissolving 100 mg of FP in 100 ml acetonitrile. Then, the solution was put in the sonicator bath Bndelinsonorexdigitec (BERLIN) For 10 min, after that, it was filtrated using 0.45 μm syringe filter. It was stored at 25°C until required. Serial dilutions were made from the stock solution using acetonitrile.

2.5 | Drug loading capacity

Drug loading was expressed using both entrapment efficiency (EnE) and encapsulation efficiency (EncE) according to Equations 1 and 2 respectively:

$$EnE\,(\%) = \frac{FP_t - FP_s}{FP_t} x\,100 \quad (1)$$

$$EncE\,(\%) = \frac{FP_Q}{Formula} x\,100 \quad (2)$$

where "FP_t", "FP_s" and "FP_Q" are the total amount of FP used in the preparation of the nanoparticles, the free amount of FP found in the supernatant upon washing and the total amount of FP quantified in each formula (FP/Tyr-PEA) respectively. FP quantification was based on the analysis of FP content in 10 mg of the final nanoparticles dissolved in 25 ml of acetonitrile using the validated HPLC method.

2.6 | Content uniformity

A HPLC measures FP content uniformity by calculating each sample's area under the curve (AUC) and then applying it to the calibration curve equation. That was done by adding (10 mg) of (FB/Tyr-PEA) to 25 ml acetonitrile. Next, the sample shaking vigorously to dissolve and placed in the sonicator for 15 min at a high altitude. After that, filtered using 0.2 μm syringe membrane filter, then injected the sample (20 μl) into the HPLC device elution was measured at 239 nm.

2.7 | Characterization of poly(ester amide) (Tyr-PEA) and FP-poly(ester amide) formula FP/Tyr-PEA

2.7.1 | Average molecular weight measurement

Molecular weight was measured in aqueous suspension by dynamic light scattering using a Nicomp N3000 (Billerica, USA)

2.7.2 | Solution viscosity

The diluted solution viscosity of the (Tyr-PEA) was measured by a dilution Ubbelohde glass capillary viscometer (Rheotek, Poulten Selfe & Lee Ltd., Essex, England) in a thermostated water bath at 25 ± 0.1°C. The solution was temperature equilibrated for 10 min before conducting measurement of viscosity. Then, the measurements were repeated until reproducible values were attained.

2.7.3 | Particle size and zeta potential analysis

The average diameter and zeta potential of the (Tyr-PEA) and (FP/Tyr-PEA) NPs were analyzed at 25°C by Photon correlation spectroscopy using a Zetasizer Nano ZS90 (Malvern Instrument, UK). Before analysis, samples were diluted with deionized water sonicated at medium amplitude (60 Hz) for 30 s. The analysis was performed in triplicate.

2.7.4 | pH sensitivity

An accurately weighed amount (0.050 g) of the produced (Tyr-PEA) was placed into several 5 ml vials, 2 ml of 1 M NaCl solution was pipetted into each vial, the vials were shaken for more than 20 h at 37°C to attain equilibrium. Then, different portions of standard aqueous 0.050 M NaOH solution in increasing volume from 0 to 1.5 ml were added. The vials were shaken for 5 h. The pH values of solutions were recorded at constant pH reading using cyberscan 510 meter calibrated with standard buffer solutions of pH = 2, 4, 7 and 10.

2.7.5 | Infrared spectroscopy (Fourier-transformed infrared spectroscopy)

Fourier-transformed infrared spectroscopy of polymer with FP, (Tyr-PEA) and (FB/Tyr-PEA) without active ingredient were recorded using Perkin Elmer FTIR spectrometer (OH, USA), coupled with Spectrum 10 software that was used to operate and treat FTIR spectra. A sample of a few milligrams was loaded on the sample holder above a laser lens and held in place by screwing down the relevant adaptor. Each sample's FTIR spectrum scans were obtained over the range of 450–4000 cm^{-1} with a resolution of 2 cm^{-1}.

2.7.6 | Nuclear magnetic resonance spectroscopy

The ^{1}H-NMR at 500 MHZ and ^{13}C-NMR at 125 MHZ of the (Tyr-PEA) were recorded on a Bruker Avance DPX 300 spectrometer (Ettlingen, Germany), tetramethylsilane (TMS) as the internal standard. Chemical shifts are recorded in ppm in relation to the internal standard. Splittings were recorded as "s" indicating singlet, "d" for doublet, "t" for triplet and finally "q" for quartet.

2.7.7 | Differential scanning calorimetry analysis

Differential scanning calorimetry (DSC) analysis of the (Tyr-PEA and FB/Tyr-PEA) NPs was carried out using DSC Q200-TA instrument (USA). A 2.5 mg sample was placed onto an aluminum pan and heated at a heating rate of 10°C/min under continuous nitrogen purging (50 ml/min).

2.7.8 | Scanning electron micrographs

Surface topography was examined (Tyr-PEA) and (FP/Tyr-PEA) NPs using JSM-IT300 (JEOL, Japan). The 2–4 mg of each sample were sprinkled on a double-adhesive carbon tape affixed to an aluminum tub. Samples were analyzed without any further coating.

2.7.9 | X-ray diffraction analysis

X-ray diffractometry (MiniFlex 600 benchtop diffractometer [RigaKu, Tokyo, Japan]) was used to investigate the physical form of (Tyr-PEA) and (FP/Tyr-PEA) NPs. The XRD experiments were performed over the range 2θ from 5 to 99°, with Cu Kα radiation (1.5148227 Å) at the voltage of 40 kV and a current of 15 mA. All samples were fixed on a glass holder and scanned in triplicate. Data were recorded at a scanning speed of 5°/min. OriginPro® software was employed to analyze the scans (OriginLab Corporation, USA).

2.7.10 | Transmission electron microscopy analysis

FP and the lyophilized powders (Tyr-PEA and FP/Tyr-PEA) were resuspended in an isotonic solution and evaluated using transmission electron microscope (TEM) (Morgagni 268D; Fei Company, Hillsboro, OR, USA). Prior to imaging, copper grids (Electron Microscopy Sciences) were placed on a droplet of the suspensions on a glass microscope slide to permit the adsorption of the particles onto the grid.

2.8 | Aerodynamic particle size analysis using next generation impactor

The in vitro deposition and aerodynamic particle size distribution analysis was accomplished using NGI (Copley

Scientific Limited Model 170, UK). A flow rate over 4 s to provide 4 L was obtained by setting the flow rate at 60 L/min. Aerosolisation performance of FP was determined using an Aerolizer® device with a size 6 capsule manually filled with 19 mg (±10%) of FP/Tyr-PEA powder. For FP, respirable dose (RD), fine particle fraction of emitted dose (FPF-ED), fine particle fraction of nominated dose (FPF- ND), and ED were determined. Samples were collected in each stage by dissolving content of each tray in 10 ml acetonitrile, the samples were then transferred to volumetric flasks and filtered using syringe membrane filter (0.2 μm filters), 20 μl of the sample were injected to the HPLC to be analyzed. All aerodynamic parameters were calculated using Formulas 3–6:

$$ED\,(\%) = \frac{\text{Cumulative content of FP from all stages X100}}{\text{Theoretical FP Content per actuation}} \tag{3}$$

$$FPF - ED\,(\%) = \frac{\text{Total amount of FP collected from trays } 2-7}{\text{Emitted dose}} \times 100 \tag{4}$$

$$FPF - ND\,(\%) = \frac{\text{Total amount of FP collected from trays } 2-7}{\text{Nominated dose per actuation}} \times 100 \tag{5}$$

$$RD\,(\mu g) = \text{Total amount of FP collected from trays } 2-7 \tag{6}$$

The MMAD was calculated based on the USP method <601.[21] the flow rate was set at 60 L/min. MMAD was calculated based on the inverse normal of the cumulative percentage under the stated aerodynamic diameter versus the log of the effective cut-off diameter of each stage of the NGI. The amount of FP that was collected from each stage from stage 1 to stage 8 was used to calculate the cumulative mass, then MMAD was calculated. All results were made in triplicates and reported as mean ± SD. Geometric standard deviation (GSD) was also calculated form the plot of the percentage of mass less than the cut-off size versus the aerodynamic diameter plotted on the logarithmic scale.

3 | RESULTS AND DISCUSSION

3.1 | Synthesis of poly(ester amide) based on tyrosine

Nonpeptidic polyamide was synthesized by amino acid tyrosine, acting as an aminophenol monomer to react with fumaryl chloride. The two reactants were polycondensed interfacially (tyrosine in water and the fumaryl chloride in chloroform). The polycondensation reaction and amide formation occur at or near the aqueous-organic interface when the two solutions are put in contact and vigorously stirred. the (Tyr-PEA) has intrinsic viscosity (0.23 dl/g) and MW 32,600 g/mol.

3.2 | Synthesis of FP loaded poly(ester amide)s based on tyrosine

Interfacial polymerization is used to create micro-nano capsules of FP drug. In interfacial polymerization, the two monomers and FP drug are dispersed in the organic and aqueous phases. The poly(ester amide) form was happening rapidly at the interface of the miniemulsions droplet by polycondensation mechanism and gave rise to the primary membrane. The reaction control was done by diffusion one from two monomers around the capsule wall.

The added value of this method (aggregates) over other carrier-based formulations is that the drug (FP) was incorporated into the polymerization process during the synthesis. Therefore, it enabled the production of a uniform blend. Upon freeze-drying, the formula is obtained as fluffy powder, which will deposit onto the lower parts of the respiratory system upon aerosolization. However, the key challenge is to blend uniformity for carrier-based formulation using course carrier lactose (marketed product). The amount of the active ingredient with lactose is low (2.1%–250 μg in 12 mg lactose), which is a pharmaceutical challenge. Further, the aggregates in this formula will be transported to the lung, while the lactose-based carriers, FP needs to detach from the surface of the carrier to settle down and deposit in the lower parts of the respiratory system. Several researchers reported that due to this, reproducibility is a major concern in the pharmaceutical industry for DPI production.[22–26]

3.3 | FP quantification and validation using HPLC analytical method

The analytical technique for the quantification of FP was formed over a concentration range of 7.8 to 125 μg/ml that produced linearity with coefficient of determination (R^2) = 0.9997. The produced regression equation was (y = 0.6022x + 0.0361) while the retention time was 4.8 min ± 0.070. The employed method was specific to FP and formulation excipients did not interfere with the peak of FP. In the produced method, the LOD and LOQ were found as 0.261 μg/ml and 0.79 μg/ml respectively.

TABLE 1 Intermediate precision and reproducibility of HPLC method to evaluate inter and intraday reproducibility (mean ± SD, $n = 3$)

Fluticasone propionate theoretical concentration (μg/ml)	Intraday % recovery (mean ± SD) ($n = 3$)	Intraday % RSD ($n = 3$)	Interday % recovery (mean ± SD) ($n = 9$)	Interday % RSD ($n = 9$)
125	98.06 ± 3.73	3.80	96.89 ± 5.58	5.76
62.5	100.00 ± 5.45	5.45	99.82 ± 6.02	6.03
31.25	99.83 ± 6.28	6.29	100.40 ± 7.00	6.97
15.625	100.55 ± 7.48	7.44	101.14 ± 7.97	7.89
7.8125	99.40 ± 10.16	10.22	96.57 ± 11.51	11.92

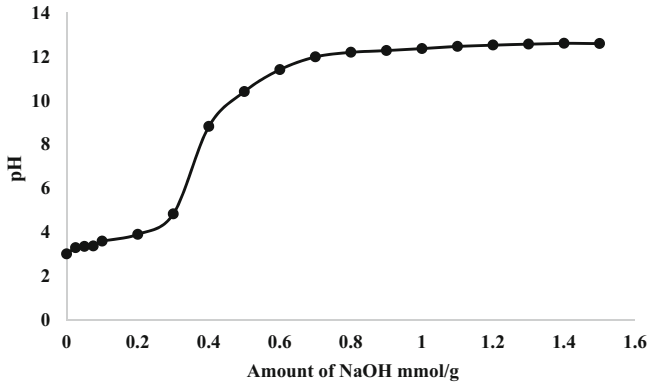

FIGURE 2 Titration curve of poly(ester amide)

Furthermore, precision of the HPLC equipment and method was evaluated by measuring 62.5 μg/ml FP standard solution 10 times. Results showed that the process was precise, with relative standard deviation (RSD) of 0.84%. The low RSD values indicate instrument precision. Accuracy of the developed method was assessed by recovery experiments, where five standard concentrations were measured in triplicates on three different days. Inter-day and intraday accuracy results are summarized in Table 1. The results demonstrated a highly accurate and reproducible process, with average recovery range from 98.06% and RSD values ranging between 3.8% and 10.2%.

3.4 | Characterization of Tyr-PEA and FP/Tyr-PEA

3.4.1 | pH sensitivity

The results pH of the prepared polymer can be obtained from the inflection point of the pH titration curve, as shown in Figure 2. The total cation exchange capacity (CEC) of a PEA specifies the amount of fixed ion-organic group in milliequivalents per gram (mq/g) of dry polymer in H-form accessible to the exchange process. For any resin, the CEC thus defined is constant, independent of experimental conditions. The CEC of the prepared PEAs from the inflection point of the pH titration curve as shown previously as pH titration curve.

3.4.2 | Particle size and zeta potential analysis

Table 2 outlines the results of zeita sizer analysis where the average particle size, polydispersity index (PDI) and zeta potential of the FP, Tyr-PEA and the FP loaded Tyr-PEA are presented. The results revealed that the employed interfacial polycondensation method resulted in nanoparticles for the polymer and the API loaded polymer within a range of 154 and 168 nm respectively. Addition of FP did not affect the particle size significantly (t- test, $p = 0.09$). The PDI indicate slight aggregation however, both the polymer and the formula possessed negative charge that exceeded −31 mV which aids deagglomeration process upon inhalation. The formed agglomerates were soft and were eorozolized easily as depicted in section 3.5.

3.4.3 | FTIR analysis

The FTIR spectra exhibit characteristic absorption bands for all organic functional groups of FP, (Tyr-PEA) and (FP/Tyr-PEA) NPs as shown in Figure 3. The FTIR spectrum of FP showed three characteristic sharp bands representing (C═O) groups at 1744 cm^{-1} corresponding to the ester carbonyl group, 1701 cm^{-1} corresponding to the thioester carbonyl 1661 cm^{-1} to the ketone carbonyl, as shown in Figure 3a. The amide group is associated with three characteristic infrared stretching absorptions. Stretching vibrations of the amide carbonyl bond appeared at 1632 cm^{-1}, and the NH bond of the amide group was observed in 3263 cm^{-1} and 1506 cm^{-1} for stretching and bending vibrations, respectively. A strong band for the carbonyl bonds stretching vibrations for carboxylic carbonyl and ester carbonyl was observed at

Material parameter	FP	Tyr-PEA	FP/ Tyr-PEA NP
Particle size (nm)	2107.2 ± 278.2	154.25 ± 22.5	167.5 ± 54.3
Polydispersity index	0.99 ± 0.18	0.41 ± 0.18	0.39 ± 0.11
Zeta potential (mV)	−18.5 ± 0.87	−31.93 ± 2.46	−31.43 ± 1.72

TABLE 2 Summary of particle size of fluticasone propionate, tyrosine poly(ester-amide) and fluticasone propionate loaded tyrosine pol(ester amide) nanoparticles (mean ± SD, $n = 3$)

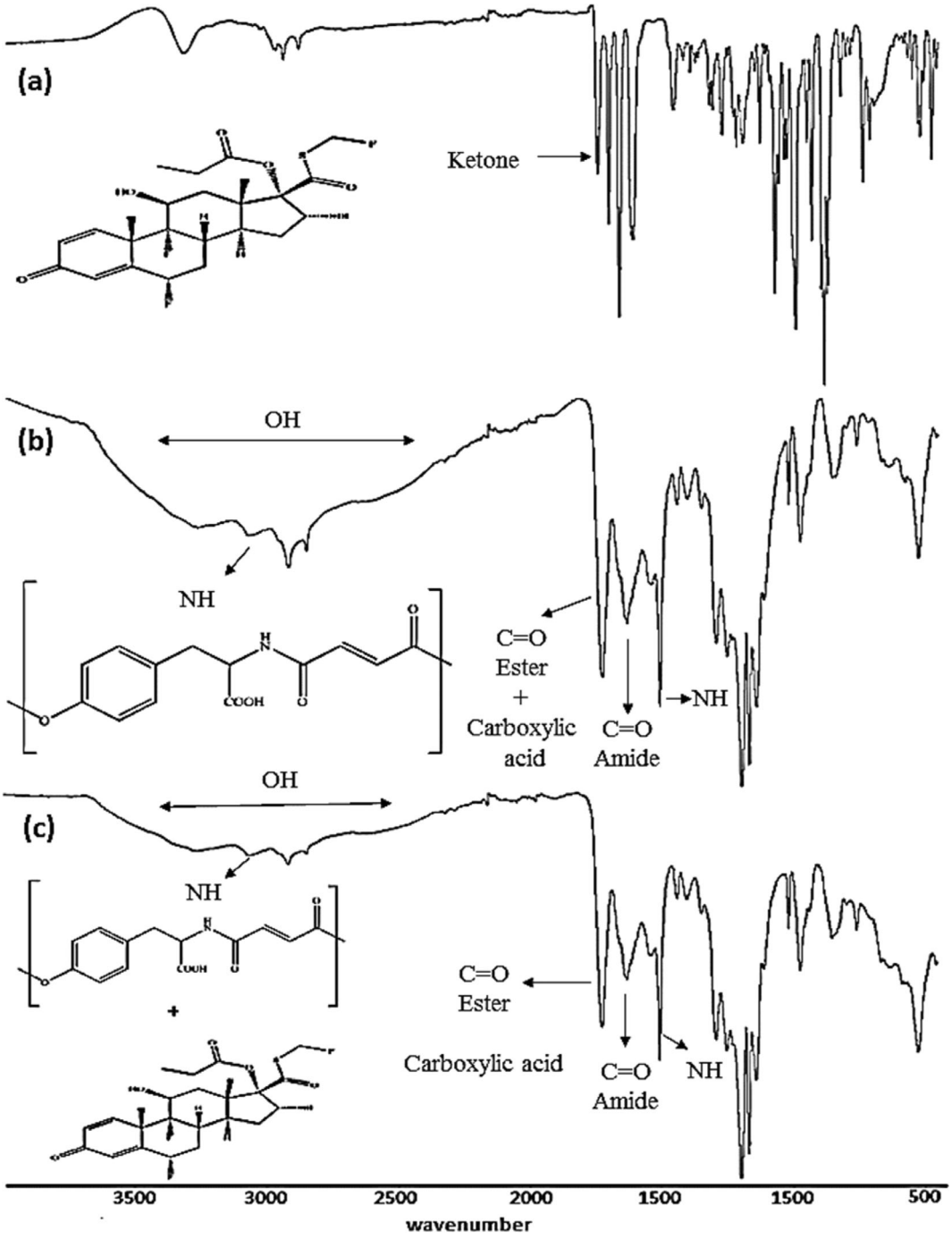

FIGURE 3 FTIR spectra of (a) fluticasone propionate (FP), (b) (Tyr-PEA) and, (c) (FP/Tyr-PEA) NPs

1725 cm^{-1}. The carboxylic acid O—H showed stretching vibrations as very broadband at 3662 to 2370 cm^{-1}. The comparison between (Tyr-PEA) and (FP/Tyr-PEA) NPs FTIR spectra shows the same characteristic bands. This may be due to the low loading of FP overlapping between the polymer and drug bands, as shown in Figure 3c.[24,27]

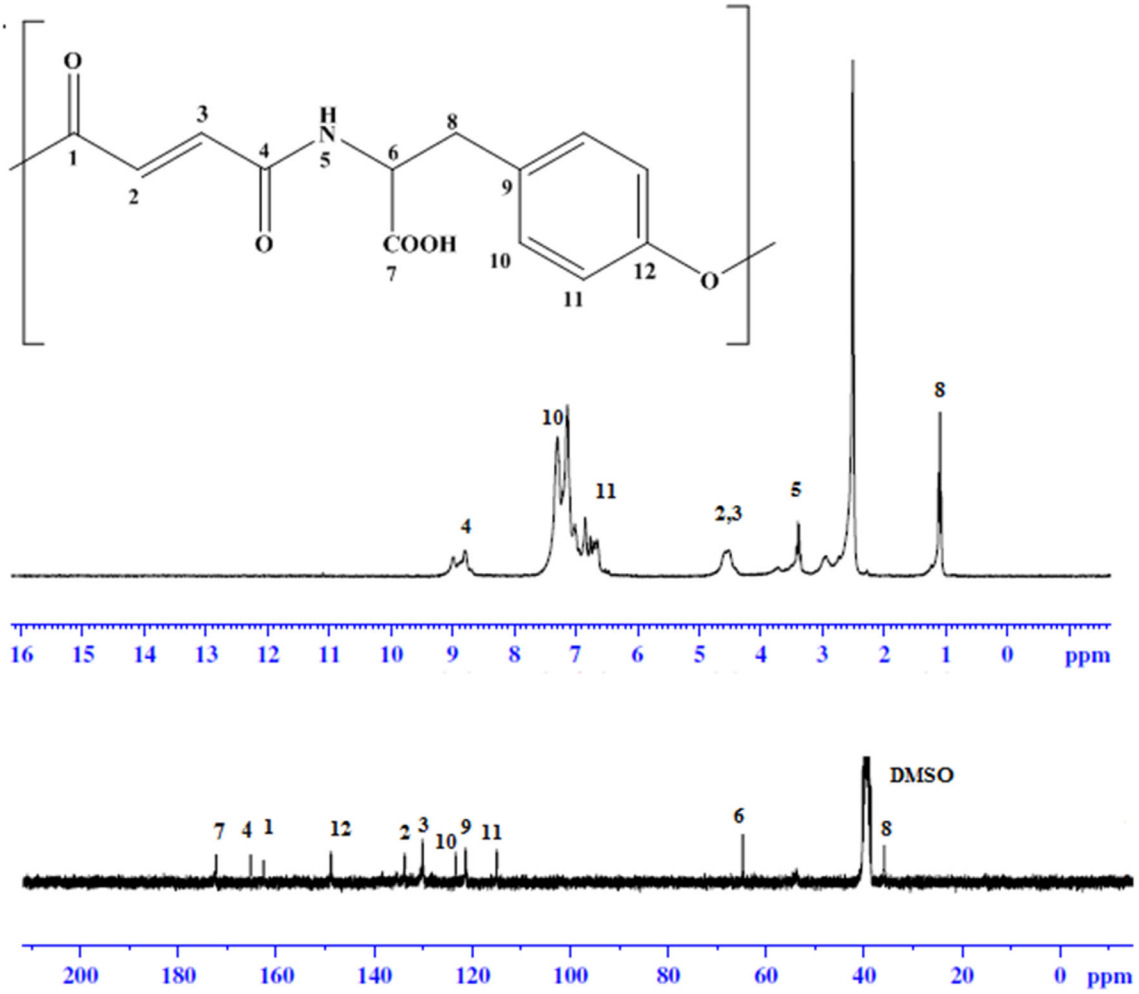

FIGURE 4 The ^{1}H NMR and ^{13}C NMR spectra [Color figure can be viewed at wileyonlinelibrary.com]

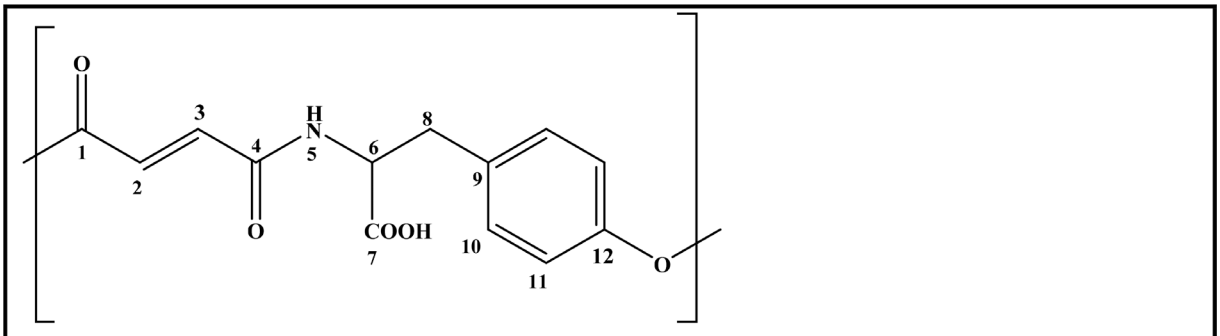

Chemical shift (ppm)

	1	2	3	4	5	6	7	8	9	10	11	12
^{1}H	-	5.57	4.51	-	8.90	3.38	-	1.09	-	6.66-7.31		-
^{13}C	165.1	135.5	130.4	162.9	-	38.6	172.5	15.9	121.2	123.2	115.0	148.1

FIGURE 5 The structure of the polymer as confirmed by ^{13}C-NMR

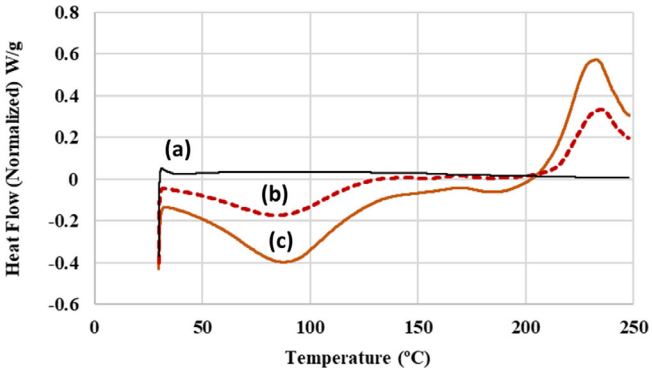

FIGURE 6 DSC profile of (a) fluticasone propionate, (b) poly(ester amide) based on tyrosine and (c) fluticasone propionate loaded poly(ester amide) [Color figure can be viewed at wileyonlinelibrary.com]

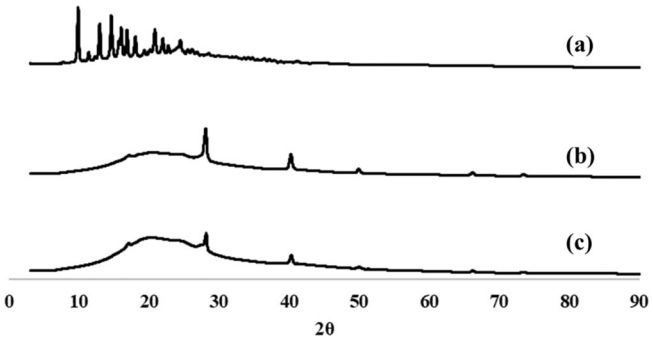

FIGURE 7 XRD curves of (a) fluticasone propionate, (b) Tyr-PEA (c) FP/Tyr-PEA

The Tyr-PEA was analyzed by ^{1}H-NMR and ^{13}C-NMR spectroscopy (Figure 4) to confirm their chemical identity and postulated the supposed product formation. The ^{1}H-NMR spectrum of the synthesized PEAs confirmed their proposed structures; a broad peak appeared at 8.90 ppm due to the proton of the amide group (-NH), multiplet peaks appeared at range 6.66–7.31 ppm that were assigned to protons of the aromatic ring of tyrosine unit. The signal for the proton of the (CH_2) group attached to the aromatic ring (Ar-CH_2) appeared as a doublet at 1.08 ppm. The signal of (CH) proton appeared as a triblet at 3.38 ppm.

The structure of the polymer was also confirmed by ^{13}C-NMR (Figure 5). The most significant feature in the ^{13}C-NMR is the characteristic peaks of the formed ester carbonyl bond at 165.1 ppm and amide carbonyl at 162.9 ppm compound. The carbons of the fumarate carbons unit were observed at 130.4 and 135.5 ppm. The benzene carbons in the tyrosine unit were observed at the range 115.0, 121.2, 123.2 and 148.1 ppm.

3.4.4 | Thermal profile

Figure 6 depicted the thermal profile of FP (Figure 6a), with a reported melting point of 261–273°C.[28,29] Therefore, the DSC thermogram could not reveal the melting point of FP as it exceeded its measurement range of the used device. As for PEA, the thermogram revealed an endothermic peak starting at 72.45°C with a peak temperature at 90.32°C indicating the glass transition of the polymer and producing an enthalpy of 7.6647 J/g. The thermogram of FP/Tyr-PEA demonstrated similar endothermic peak with an onset at 65.67°C and a peak at 88.05°C producing an enthalpy of 19.907 J/g. Such an increase in enthalpy could be attributed to the encapsulation of FP within the polymer chains. Similar results were reported earlier.[30]

3.4.5 | XRD analysis

XRD analysis of FP, the Tyr-PEA and FP/Tyr- PEA are presented in Figure 7. FP showed a characteristic diffraction peaks between 10 and 30 2θ indicating the crystalline nature of the active ingredient (Figure 7a). As for Tyr-PEA (Figure 7b), the XRD pattern demonstrated a semi crystalline material with few sharp peaks at 28 and 40.4 2θ and a wide broad heep between 10 and 25 2θ. The same peaks were presented in the FP/Tyr-PEA nanoparticles (Figure 7c). Similar results were reported regarding the semicrystalline nature of PEA.[31] However, none of FP peaks were present in the FP-PEA nanoparticles spectra indicaing either an inclusion of FP within the polymer or a possible transformation of the drug into an amorphous material. Similar results were also reported in.[24]

3.4.6 | SEM analysis

SEM images as can be seen from Figure 8 highlighted the aggregates of the FP/Tyr-PEA. Also, the figure revealed the presence of pores within the aggregates (Figure 8d–f) which is favorable for respiratory delivery of powders. Duong and coworkers reported the importance of porous materials for DPI formulations due to better aerodynamic performance, and provision of Large surface area.[32] ImageJ analysis of 50 aggrates revealed an average particles size of 3.07 ± 1.02 μm. Such results supports the aerodynamic performance analysis. Effective DPI is when particles and aggregates are within the size range of 1–5 μm.[33]

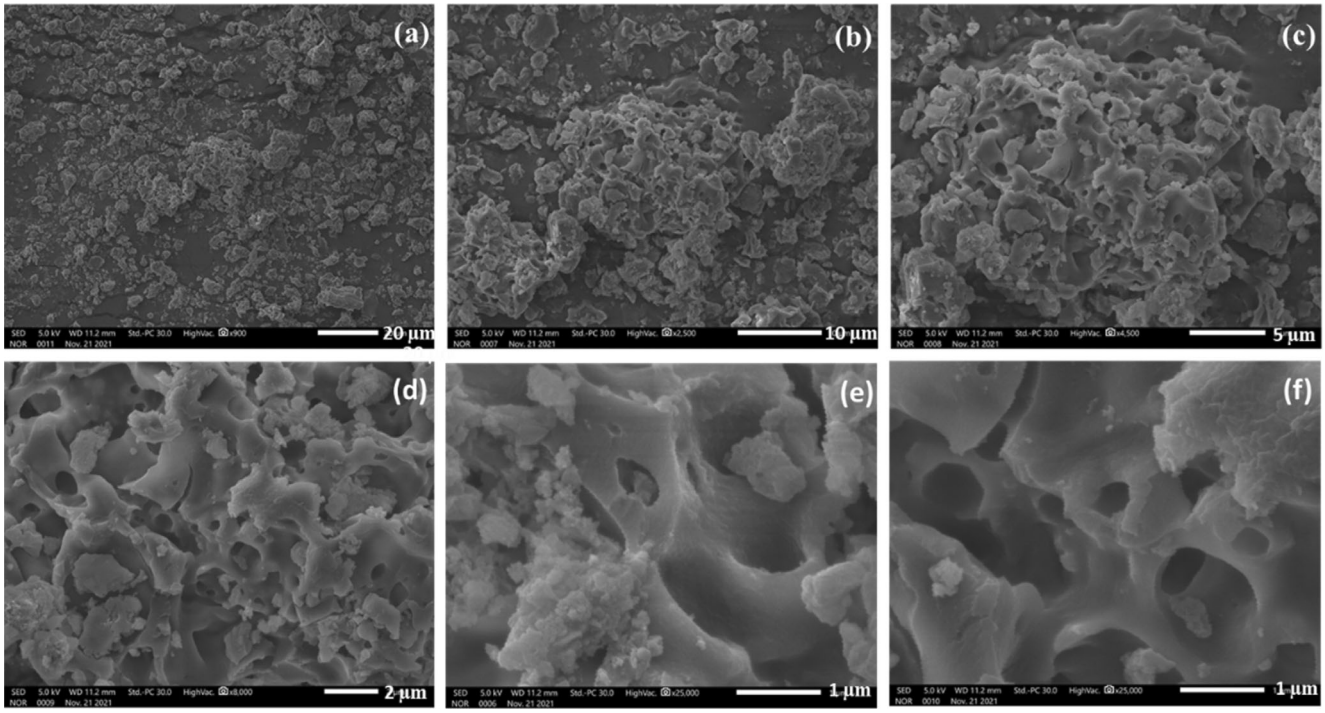

FIGURE 8 SEM images of fluticasone propionate loaded poly(ester amide) (FP/Tyr-PEA) formula at various magnifications (a) 900×, (b) 2500×, (c) 4500×, (d) 8000×, (e) 25,000×, and (f) 25,000, highlighting porous aggregates

3.4.7 | TEM analysis

TEM analysis as can be seen from Figure 9 confirmed the spherical nanoparticles with size ranging from 31 to 60 nm. The particles are present as nanoaggregates which furnishes pulmonary drug delivery and deposition towards the lower parts of the lung.[24] It is proposed that upon inhalation, the nanoaggregates will disintegrate into their primary nanoparticles. ImageJ software analysis of 80 particles revealed an average particle size of 45.39 ± 6.32 nm. The size obtained here is smaller than that obtained by the laser diffraction and this could be attributed to the formation of hydrated layer around the particles and/or the presence of aggregates.[34,35]

3.5 | In-Vitro assessment of the aerodynamic performance of the formula (polymer contain FP) using NGI

The produced particles upon freeze drying demonstrated a fluffy powder. Such particles were assessed for aerodynamic performance and compared to the marketed product (FP, DPI with 250 µg/actuation). F1 formula is based on aggregates formulation using the Tyr-PEA as a carrier. While the marketed product is based on blending with a carrier (lactose). The content uniformity of the produced polymer was calculated based on encapsulation efficiency results. Overall the produced formula entrapped 92.32% of FP and the encapsulation efficiency was reported to be 0.526% (i.e., each 19 mg of the FP/Tyr-PEA powder contained the required 100 µg of FP). Five samples of the final formula were analyzed for content uniformity and results were 98.91% ± 1.24% ($n = 5$). Therefore, each capsule was filled with 19 mg of the FP/Tyr-PEA.

The aerodynamic performance of the formulation was assessed using the NGI. Results are depicted in Figure 10 which highlighted the main aerodynamic parameters. The ED of the produced formulation was 87.29% while that for the marketed product did not exceed 59%. Formula 1 (F1) which contain Tyr-PEA with FP produced higher respirable dose when compared to the marketed FP dry powder inhaler (48.63 µg vs. 34.15 µg) despite lower initial content. The difference between F1 and the marketed product in terms of ED and RD was statistically significant (t-test, $p < 0.05$). Similarly F1 produced higher FPF-ND and FPF-ED when compared with the marketed product. However, the selection of the 250 µg per puff marketed product was based on local availability.

The MMAD (Table 3) which represents the mean aerodynamic particle size for F1 and marketed product were similar with no significant difference between them (t-test $p > 0.05$). This is a favorable size for pulmonary drug delivery of inhaled powders.[22] Typical inhalation products generate aerosols with the expected MMAD in

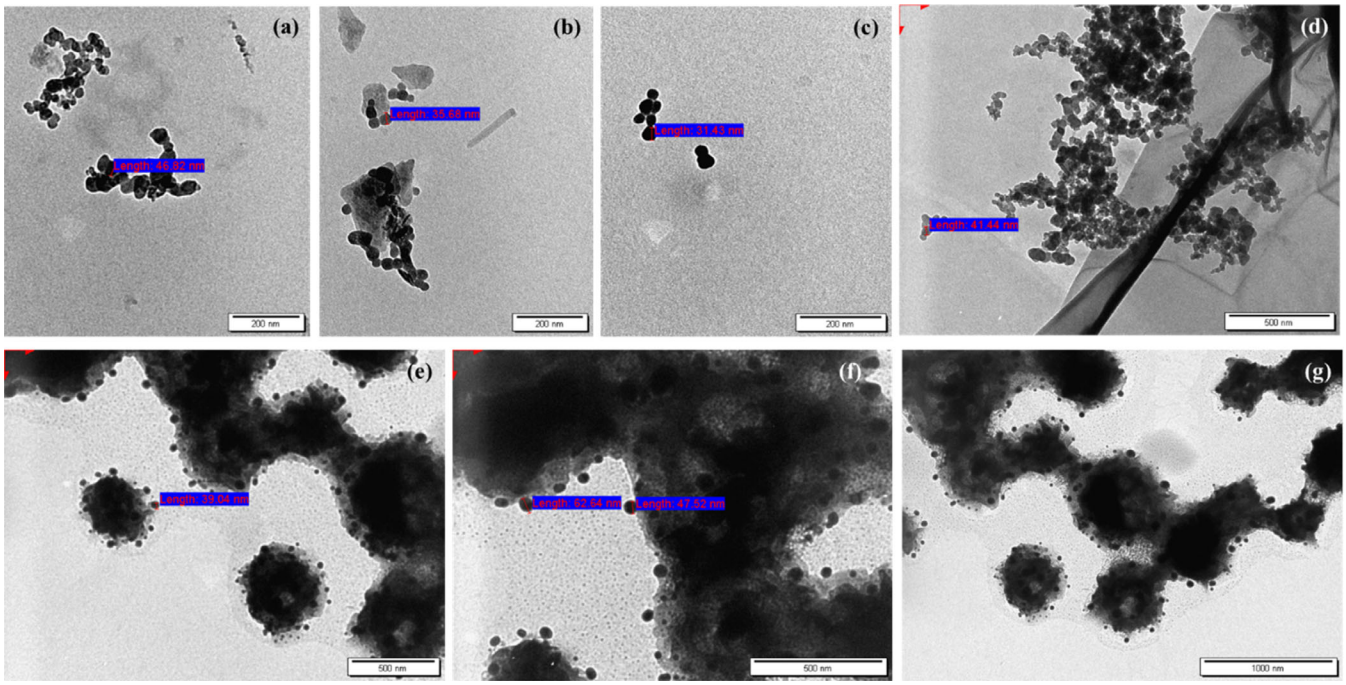

FIGURE 9 TEM images of FP/Tyr-PEA formula at various magnifications highlighting the presence of nanoaggregates [Color figure can be viewed at wileyonlinelibrary.com]

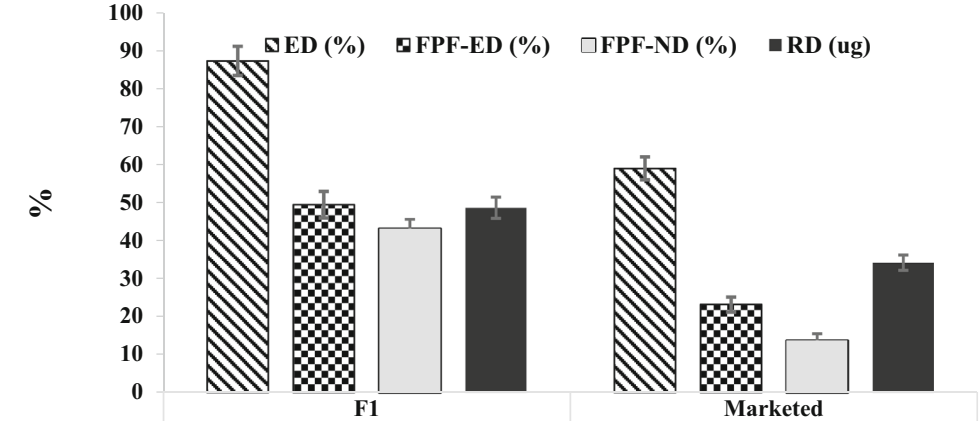

	F1	Marketed
ED (%)	87.29	58.99
FPF-ED (%)	49.42	23.16
FPF-ND (%)	43.09	13.60
RD (ug)	48.63	34.15

FIGURE 10 Summary of in-vitro aerodynamic performance of FP using NGI. F1: each capsule contains 19 mg of the formula with FP content of 100 μg carried by polymer. Marketed: actuation contains 250 μg of FP. Results are presented as mean ± SD, $n = 3$. ED, % emitted dose; FPF-ED, fine particle fraction from emitted dose; FPF-ND, fine particle fraction from nominated dose; RD, respirable dose

the range of 1.5–3.5 μm to optimize the drug dose which penetrates to the lung.[22,36,37]

Further examination of individual stage deposition of the formulation and the marketed product as can be seen from Figure 11a showed that both formulations had extra-thoracic deposition of a total 50.64% and 76.84% for F1 and the marketed product, respectively. However, the extra thoracic deposition of F1 is less than that of the marketed FP DPI. Similarly, both formulations had no extrapulmonary deposition of FP. Representative figures of the particles deposition on individual trays within the NGI can be seen in Figure 11b and Figure 11c for F1 and the marketed product, respectively.

TABLE 3 MMAD and GSD of F1 and the Marketed product

Formulation	MMAD (μm)	GSD
F1	1.455	0.075
Marketed product	1.434	0.074

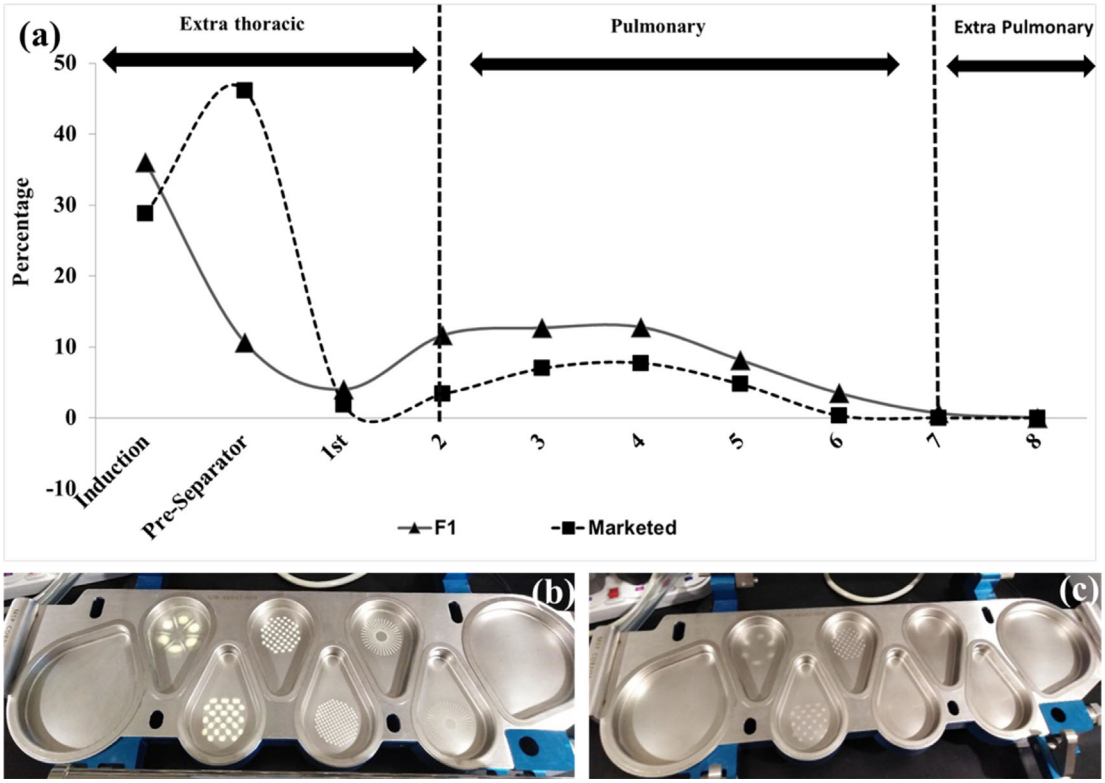

FIGURE 11 (a) In vitro comparison of aerodynamic particle size distribution of the F1 demonstrating the lung deposition of FP using NGI set at flow rate of 60 L/min, (b) Deposition of the FP aggregates (F1) onto the NGI apparatus highlighting the powder on tray 1–7, (c) Deposition of the market product onto the NGI apparatus highlighting the white powder from tray 1–7 [Color figure can be viewed at wileyonlinelibrary.com]

4 | CONCLUSIONS

FP-loaded-tyrosine based poly(ester amide) nanoaggregates were successfully prepared using interfacial polymerization technique. The optimized inhalable formulation has demonstrated favorable properties. Characterization techniques revealed the production of nanoaggregates capable of delivering a respirable dose of FP of 48.63 μg in comparison with 34.15 μg of the marketed product. The morphological analysis showed that the particles were spherical aggregates with primary size of 45.39 ± 6.32 nm. The employed interfacial polymerization technique based on amino acid enabled the production of a simple, cost-effective biodegradable and biocompatible alternative to the development of dry powder inhaler formulation.

AUTHOR CONTRIBUTIONS

Dalia K. Ali: Data curation (supporting); formal analysis (equal); methodology (supporting); project administration (supporting); supervision (equal); writing – original draft (equal); writing – review and editing (supporting). **Hamad S. Alyami:** Data curation (supporting); investigation (supporting); writing – review and editing (supporting). **Esra' Taybeh:** Project administration (supporting); supervision (supporting); writing – original draft (supporting); writing – review and editing (supporting). **Shereen M. Assaf:** Conceptualization (supporting); project administration (supporting); writing – review and editing (supporting). **Eman Zmaily Dahmash:** Conceptualization (lead); formal analysis (equal); methodology (equal); project administration (supporting); supervision (equal); writing – original draft (equal); writing – review and editing (equal).

ACKNOWLEDGMENTS

The authors would like to acknowledge the funding from Isra University (Jordan) for funding Hussien Abdulakarim towards his MSc.

CONFLICT OF INTEREST

All authors declare no conflict of interest.

DATA AVAILABILITY STATEMENT

The data that support the findings of this study are available from the corresponding author upon reasonable request.

ORCID

Dalia K. Ali https://orcid.org/0000-0001-9680-0026
Esra' Taybeh https://orcid.org/0000-0001-7493-7865
Hamad S. Alyami https://orcid.org/0000-0003-3513-4976
Shereen M. Assaf https://orcid.org/0000-0002-3888-9330
Eman Zmaily Dahmash https://orcid.org/0000-0002-9815-3720

REFERENCES

[1] L. S. Nair, C. T. Laurencin, *Tissue Eng.* **2005**, *1*, 47.
[2] J. Park, M. Ye, K. Park, *Molecules* **2005**, *10*, 146.
[3] Y. Ikada, H. Tsuji, *Macromol. Rapid Commun.* **2000**, *21*, 117.
[4] J.-M. Lü, X. Wang, C. Marin-Muller, H. Wang, P. H. Lin, Q. Yao, C. Chen, *Expert Rev. Mol. Diagn.* **2009**, *9*, 325.
[5] G. Tsitlanadze, T. Kviria, R. Katsarava, *J. Mater. Sci. Mater. Med.* **2004**, *15*, 185.
[6] A. C. Fonseca, J. F. J. Coelho, J. F. A. Valente, T. R. Correia, I. J. Correia, M. H. Gil, P. N. Simões, *J. Biomater. Sci. Polym. Ed.* **2013**, *24*, 1391.
[7] P. Karimi, A. S. Rizkalla, K. Mequanint, *Materials (Basel).* **2010**, *3*, 2346.
[8] E. Marin, M. I. Briceño, C. Caballero-George, *Int. J. Nanomed.* **2013**, *8*, 3071.
[9] C. P. Reis, R. J. Neufeld, A. J. Ribeiro, F. Veiga, I. Nanoencapsulation, *Nanomed. Nanotechnol. Biol. Med.* **2006**, *2*, 8.
[10] K. S. Soppimath, T. M. Aminabhavi, A. R. Kulkarni, W. E. Rudzinski, *J. Controlled Release* **2001**, *70*, 1.
[11] M. Rawat, D. Singh, S. Saraf, S. Saraf, *Biol. Pharm. Bull.* **2006**, *29*, 1790.
[12] M. Smola, T. Vandamme, A. Sokolowski, *Int. J. Nanomed.* **2008**, *3*, 1.
[13] E. Hossny, N. Rosario, B. W. Lee, M. Singh, D. El-Ghoneimy, J. Y. Soh, et al., *World Allergy Org. J.* **2016**, *9*, 26.
[14] C. Loira-pastoriza, J. Todoroff, R. Vanbever, *Adv. Drug Delivery Rev.* **2014**, *75*, 81.
[15] (GINA) GIFA. Global strategy for asthma management and prevention. **2019**.
[16] P. Chanez, A. Bourdin, I. Vachier, P. Godard, J. Bousquet, A. M. Vignola, *Proc. Am. Thorac. Soc.* **2004**, *1*, 184.
[17] P. Muralidharan, M. Malapit, E. Mallory, D. Hayes, H. M. Mansour, *Nanomed. Nanotechnol. Biol Med.* **2015**, *11*, 1189.
[18] Y. Yang, N. Bajaj, P. Xu, K. Ohn, M. D. Tsifansky, Y. Yeo, *Biomaterials* **2009**, *30*, 1947.
[19] A. R. S. Couto, D. E. Cardoso, H. M. Cabral-Marques, *Sci. Pharm.* **2014**, *82*, 787.
[20] ICH. International Conference on Harmonisation of Technical Requirements for Registration of Pharmaceuticals for Human Use. Validation of Analytical Procedures: Text and Methodology Q2(R1). Version 4, 2005. Online. (accessed: 20 September 2022).
[21] USP-35. The United States pharmacopeia: the National Formulary: USP 35 NF 30th Edition. Authority of the United States Pharmacopeial Convention I. Washington, D.C. Rockville **2011**.
[22] B. K. Nanjwade, S. A. Adichwal, K. R. Gaikwad, K. A. Parikh, F. V. Manvi, *PDA J. Pharm. Sci. Technol.* **2011**, *65*, 513.
[23] E. Z. Dahmash, D. K. Ali, H. S. Alyami, H. Abdulkarim, M. H. Alyami, A. H. Aodah, *Polymers (Basel).* **2022**, *14*, 1082.
[24] M. H. Alyami, E. Z. Dahmash, D. K. Ali, H. S. Alyami, H. AbdulKarim, S. A. Alsudir, *Pharmaceuticals* **2022**, *15*, 321.
[25] D. A. Wyatt, J. S. Koner, E. Z. Dahmash, A. R. Mohammed, *J. Aerosol. Med. Pulmonary Drug Delivery* **2019**, *32*, A18.
[26] J. S. Koner, D. Wyatt, S. Lungare, R. Jones, A. R. Mohammed, *J. Aerosol. Med. Pulmonary Drug Delivery* **2020**, *33*, A3.
[27] D. K. Ali, A. M. Al-zuheiri, B. A. Sweileh, International Journal of Polymer Analysis and pH and reduction sensitive bio-based polyamides derived from renewable dicarboxylic acid monomers and cystine amino acid. **2017**, 5341.
[28] R. Westmeier, H. Steckel, *J. Pharm. Sci.* **2008**, *97*, 2299.
[29] PubChem. Fluticasone Propionate. **2022**. https://pubchem.ncbi.nlm.nih.gov/compound/Fluticasone-propionate
[30] R. Surekha, T. Sumathi, *Int. J. Pharm. Clin. Res.* **2016**, *8*, 1616.
[31] S. Ion, *Rev. Roum. Chim.* **2009**, *54*, 381.
[32] T. Duong, C. López-Iglesias, P. K. Szewczyk, U. Stachewicz, J. Barros, C. Alvarez-Lorenzo, M. Alnaief, C. A. García-González, *Front Bioeng. Biotechnol.* **2021**, *9*, 671381.
[33] A. Chvatal, Á. Farkas, I. Balásházy, P. Szabó-Révész, R. Ambrus, *Int. J. Pharm.* **2017**, *520*, 70 https://www.sciencedirect.com/science/article/pii/S0378517317300790
[34] S. Hu, L. Sun, M. Liu, H. Zhu, H. Guo, H. Sun, H. Sun, *New J. Chem.* **2015**, *39*, 4568.
[35] Y. Zhu, Y. Fang, L. Borchardt, S. Kaskel, *Microporous Mesoporous Mater.* **2011**, *141*, 199.
[36] L. Gradon, T. R. Sosnowski, *Adv. Powder Technol.* **2014**, *25*, 43 https://www.sciencedirect.com/science/article/pii/S0921883113001921
[37] T. R. Sosnowski, *J. Nanosci. Nanotechnol.* **2015**, *15*, 3476.

How to cite this article: H. AbdulKarim, D. K. Ali, E. Taybeh, H. S. Alyami, S. M. Assaf, E. Z. Dahmash, *J. Appl. Polym. Sci.* **2023**, *140*(13), e53672. https://doi.org/10.1002/app.53672